Circularly polarized integrated filtering antenna with polarization reconfigurability

Yunlong Lu[1,4*], Yi Wang[2*], Steven Gao[3], Changzhou Hua[1], and Taijun Liu[1]

[1] Faculty of Electrical Engineering and Computer Science, Ningbo University, Ningbo, Zhejiang, 315211, China
[2] Department of Engineering Science, University of Greenwich, ME4 4TB, Kent, UK
[3] School of Engineering and Digital Arts, University of Kent, Canterbury CT2 7NZ, U.K.
[4] State Key Laboratory of Millimeter Waves, Southeast University, Nanjing 210096, China.
[*] yi.wang@greenwich.ac.uk

Abstract: A new design of circularly polarized (CP) integrated filtering antennas with reconfigurable polarization is proposed in this paper. Two phase-reconfigurable coupled λ/2-resonator pairs have been used to feed the antenna and generate the 2nd-order filtering response and the circular polarization simultaneously. By switching the PIN diodes inserted in the feeding network, a phase difference of +90° or - 90° can be realized at the outputs of the feeding network. This renders the antenna's capability of switching its polarization from right hand circular polarization (RHCP) to left hand circular polarization (LHCP) or vice versa. The use of the coupled-resonator pairs significantly improves the frequency selectivity and out-of-band rejection of the CP antenna. To the best of the authors' knowledge, this is the first report of a multifunctional antenna which has integrated filtering performance, circular polarization and polarization reconfigurability. To verify the design concept, a reconfigurable CP antenna operating at 2.45 GHz is implemented. The simulated and measured results agree well with each other and show that the antenna has an impedance bandwidth of 4.5 %, an average in-band gain of 6.0 dBic (LHCP)/6.1 dBic (RHCP), out-of-band rejections of greater than 10.8 dB, and 3-dB AR bandwidth of 9.4 %/10.5 %.

1. Introduction

Circular polarization (CP) reconfigurable antennas have received increasing attention, as they can serve many purposes such as enhancing the system capacity, mitigating the multi-path fading in wireless channels, and reducing the polarization mismatching between transmitting and receiving antennas [1-3]. Many efforts have been made on reconfigurable CP antennas [4-10]. One approach is to reconfigure the radiating elements. RF switches such as PIN diodes and RF-MEMS, loaded on E-/L- shaped patches [4, 5] or slots etched in the patches [6, 7], have been used to alter the effective radiating structure for different polarizations. The other popular approach is to reconfigure the feeding networks [8-11]. This can be achieved by controlling the phases feeding into the radiation element using RF switches. For instance, an annular ring antenna fed by a reconfigurable transmission line was demonstrated in [8]. A circular and a ring patch fed by a reconfigurable feeding network were presented in [9] and [10], respectively. In [11], a wideband circular polarized reconfigurable antenna, consisting of four radiating arms with sequential excitations, also adopted a reconfigurable feeding network.

The bandpass filter (BPF) is another key component in RF front-ends. With the rapid development of modern microwave systems, microwave devices with multiple integrated functions are in increasing demand. The co-design of filtering antennas with integrated filtering and radiation functions is of great interest, as the integration offers more compact structures and enhanced overall performance by eliminating the 50 Ω interfaces between the antenna and filter in the traditional cascaded configuration [12].

The past few years have witnessed a lot of efforts on the co-design of filters and antennas [13-17]. One straightforward but less integrated approach is to cascade the filtering circuit with an antenna and use an additional impedance transformer to achieve the matching between them [13]. A truly seamless integration scheme is to replace the last-stage resonator of a filter with a resonant radiator [14, 15], where the resonant antenna forms one pole of the filter and contributes to its frequency selectivity [16, 17]. The above-mentioned only concerns linear polarization antennas. For circular polarization antennas, the design involves more sensitive parameters to be optimized. Therefore the integration of filtering functions in CP antennas becomes even more challenging. Very little work about this has been done in the literature. In [18], a linear-to-circular polarization transformer was embedded in a horn antenna, also serving a filtering function. In [19], a narrow band and a wideband filtering CP antenna were designed by integrating the filtering circuits into a single-feed or a dual-feed feeding network, respectively. To the best of the authors' knowledge, no CP antennas have been demonstrated with an integrated filtering function as well as reconfigurable polarization in the literature.

In this paper, a novel reconfigurable filtering CP antenna is proposed. The integrated filtering function is achieved by using two coupled λ/2-resonator pairs, whereas the reconfigurability is realized in the feeding network using PIN diodes. The unique phase properties of the coupled λ/2-resonator pairs have been utilized to feed the patch to generate circular polarization. By changing the tapping positions of the I/O ports to the coupled resonator pair, the output phase can be switched between -90° and +90°. At the same time, the amplitude characteristics of the coupled resonator pairs renders the filtering responses. For the

reconfigurability, by combining 90° phase shifters and PIN diodes, the phase differences at the outputs of the feeding network can be electrically tuned from -90° to +90°. Hence, the proposed CP antenna exhibits the filtering response and reconfigurable polarization simultaneously. For demonstration, a CP antenna at 2.45 GHz is designed, fabricated and measured. Good agreement between the simulated and measured results validates the proposed design concept.

2. Design and analysis

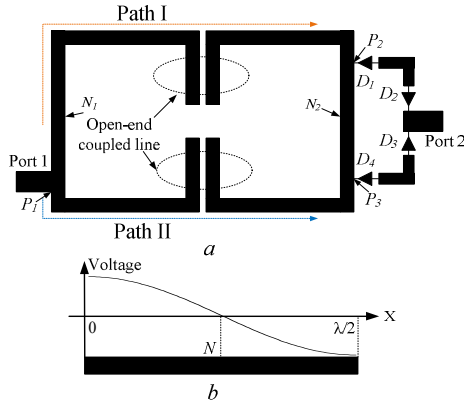### 2.1. Phase-Reconfigurable Filtering Structure

Fig. 1. *The reconfigurable coupled resonator pair (a)* Circuit layout, *(b)* Voltage-wave distribution along an ideal $\lambda/2$-resonator

To obtain the filtering response and polarization switching between left hand circular polarization (LHCP) and right hand circular polarization (RHCP), a phase-reconfigurable filtering structure is used as shown in Fig. 1. It consists of a coupled $\lambda/2$-resonator pair and four PIN diodes. The PIN diodes, grouped into D_1, D_2 and D_3, D_4, are utilized to control the tapped position of Port 2. When the diodes D_1, D_2 are ON and D_3, D_4 OFF, Port 2 is tapped to the position P_2. Conversely, it is onto P_3.

As illustrated from the voltage-wave distribution in a $\lambda/2$-resonator in Fig. 1b, a phase shift of 180° occurs when the signal passes through the voltage minimum point N. Between every two consecutive voltage minima, the phase remains the same [20, 21]. For the circuit in Fig. 1a, N_1 and N_2 are the voltage minima. So, at the two tapping positions, P_2 and P_3 situated on the opposite side of N_2, their phase difference is 180°. In the coupled $\lambda/2$-resonator pair, there are two coupling paths, Path I and II, between Port 1 and 2. Suppose the phase reference is 0° at the position P_1 of Port 1, and the PIN diodes are configured to select the tapped positon P_2 at Port 2. Both paths contain one voltage minimum and one open-end coupled line section. Hence, the phase shifts of both paths are -90°. Consequently, the phase shift between P_1 and P_2 remains -90°. In contrast, if the tapped position P_3 is selected, Path I contains two voltage minima (N_1 and N_2) and one open-end coupled line section, whereas Path II only has one open-end coupled line section. The phase shifts of both paths are +90° [22].

As a result, the phase difference between the input and output ports can be controlled to be either -90° or +90° by switching the PIN diodes. Meanwhile, the amplitude
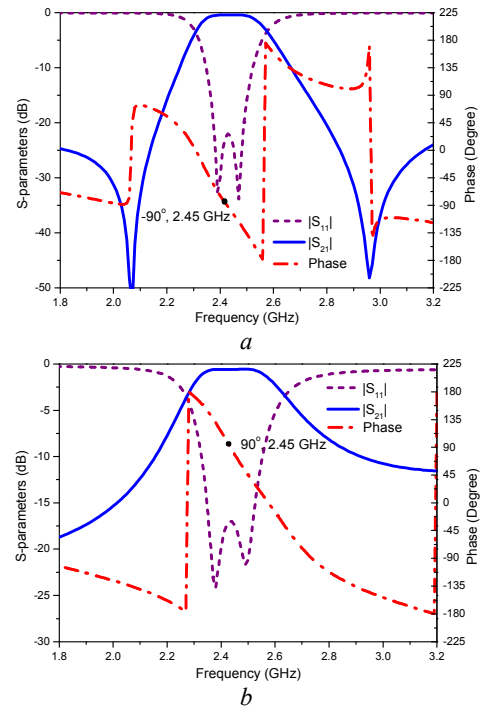

Fig. 2. *Simulated amplitude and phase responses of the phase-reconfigurable filtering structure (a)* State I: D_1, D_2 ON and D_3, D_4 OFF, *(b)* State II: D_1, D_2 OFF and D_3, D_4 ON

responses of the coupled $\lambda/2$-resonator pair exhibit filtering characteristics. The simulated amplitude and phase responses are shown in Fig. 2. For D_1, D_2 ON and D_3, D_4 OFF (State I), the phase shift is -90° at the center frequency. For D_1, D_2 OFF and D_3, D_4 ON (State II), the phase shift is 90° at the same frequency. The phase property of the coupled $\lambda/2$-resonator pair makes it a J-inverter that can be matched to any impedance, which is useful for impedance matching in antenna designs. It can be seen that two transmission zeros appear in State I. They are created by the two unequal arms from the tap points to the ends of the $\lambda/2$-resonators that are roughly quarter of a guided wavelength at the two zeros. Interestingly no transmission zeros are observed in S_{21} of Case II when the I/O take a non-diagonal configuration, as was also observed in [23].

2.2. Configuration and Operation Principle of the Proposed CP Antenna

The configuration of the proposed CP patch antenna is illustrated in Fig. 3. It consists of two substrates (Substrate #1 and Substrate #2) stacked together using four plastic screws. The two substrates have the same sizes of $L_s \times L_s$ and are separated by h. The radiation patch lies on the top layer of Substrate #1, and the reconfigurable feeding network and its ground plane are printed on the top and bottom layers of the Substrate #2. The patch is fed by two probes connected to the reconfigurable feeding network. All the substrates are Rogers 4350B, with a relative permittivity ε_r of 3.48, the thickness h_1 of 0.762 mm, and the loss tangent of 0.002. All simulations are performed using HFSS.
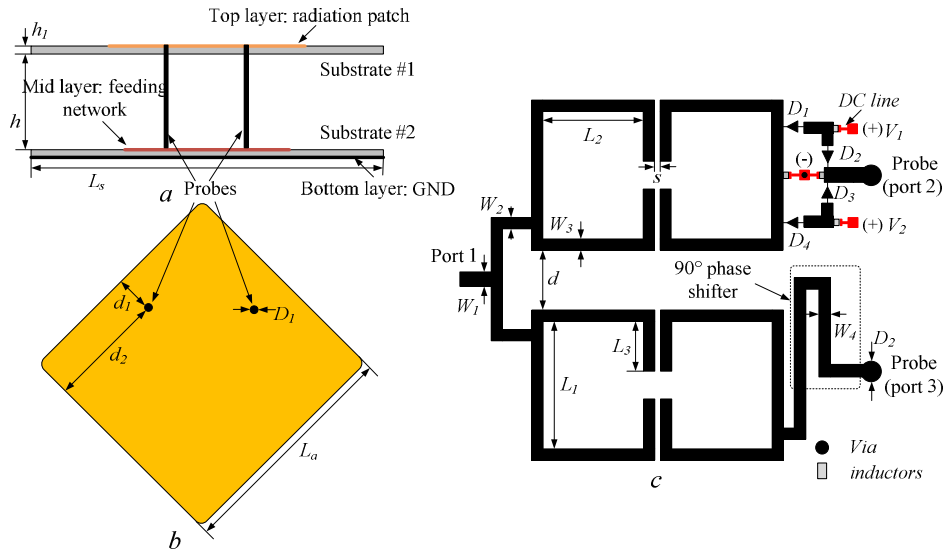
Fig. 3. *Configuration of the proposed filtering CP antenna.*
(a) Side view, *(b)* Radiation patch, *(c)* Reconfigurable feeding network

Table 1 Polarizations at different states of PIN diodes

DC (V_1)	DC (V_2)	States	PIN diodes	Polarizations
3 V	0	I	D_1, D_2 ON, D_3, D_4 OFF	LHCP
0	3 V	II	D_1, D_2 OFF, D_3, D_4 ON	RHCP

Table 2 Design parameters (mm)

L_s=80	h=10	h_1=0.762	D_1=1.28	L_a=43
L_1=9.45	L_2=9.45	L_3=3.225	W_1=1.68	W_2=0.93
W_3=0.8	W_4=0.55	s=0.65	d=10	d_1=9.2
d_2=25.2	D_2=2.2			

in Fig. 1*a*, a dual-feed feeding network for the CP antenna is constructed as shown in Fig. 3c. One phase-reconfigurable filtering structure and one fixed coupled $\lambda/2$-resonator pair cascaded with a 90° phase shifter are used, with their outputs connected to the probes to the patch antenna. Skyworks SMP1345-079LF PIN diodes with a small capacitance (less than 0.2 pF) and series resistance (2 Ω) are chosen in this prototype. The DC bias voltages V_1 and V_2 are used to turn ON or OFF the PIN didoes. The DC wires and the grounded via are isolated from the RF signal by 47 nH inductors. When V_1 is a positive voltage (3 V), the PIN diodes are set to State I, whereas when V_2 is 3 V, the PIN diodes are configured to State II. So the tapped position of Port 2 can be switched according to the ON/OFF states of the PIN diodes. The phase shift of +90° or -90° is obtained at Port 2. The 90° phase shifter added before Port 3 is to fix the phase between Port 1 and 3 to be 0°. Therefore, the phase difference between Port 2 and 3 can be electrically switched between +90° and -90°, which leads to a polarization switch between LHCP and RHCP. The relationship between the polarization and the PIN diodes is summarized in Table 1, and the detailed dimensional parameters are given in Table 2.

The simulation results of the reconfigurable feeding network are shown in Fig. 4. For State I, the phase difference between Port 2 and 3 at the center frequency of 2.45 GHz is 90°, as shown in Fig. 4*a*. Over the bandwidth from 2.15 GHz to 2.62 GHz, this difference is 93° ± 6°. To obtain the -90° phase difference at the center frequency, the PIN diodes are configured to State II. The phase difference over the bandwidth from 2.08 GHz to 2.67 GHz is -91° ± 5° as shown in Fig. 4*b*. For the amplitude responses, both states exhibit the characteristics of a 2nd-order filtering power
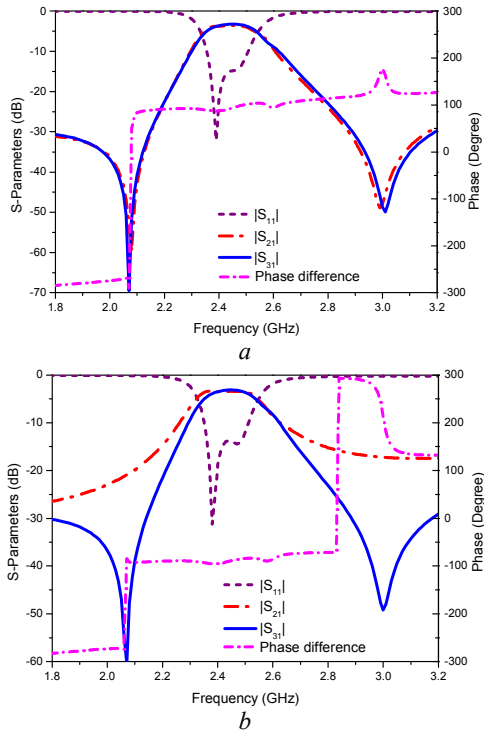

Fig. 4. *Simulation results of the reconfigurable feeding network in Fig. 3c*
(a) State I, *(b)* State II

Based on the phase-reconfigurable filtering structure

divider. The simulated insertion losses are 3.73 dB and 3.76 dB for State I and II, respectively, and the amplitude imbalances are within 0.3 dB. With these amplitude and phases feeding to the patch, the LHCP or RHCP mode can be achieved. Fig. 5 shows the current distributions on the patch over one time period under different PIN diode states. As expected, the surface current rotates clockwise under State I indicating a LHCP in Fig. 5a. In contrast, when the PIN diodes are set to State II, the surface current rotates anti-clockwise, as shown in Fig. 5b, leading to a RHCP mode.
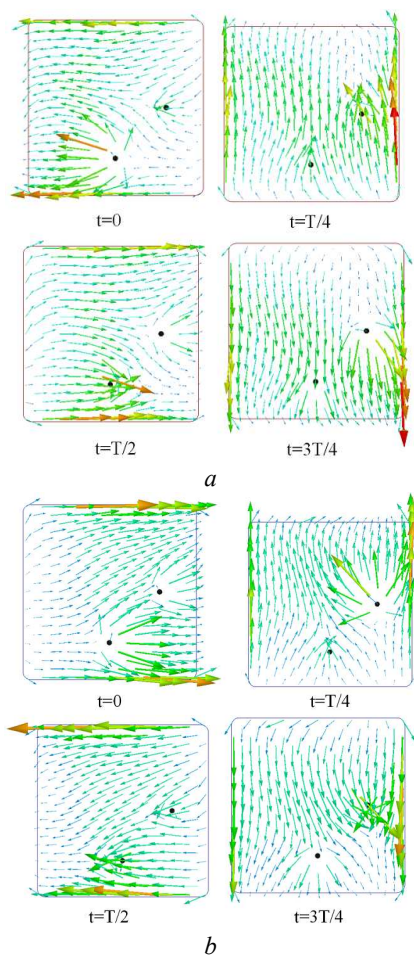

t=0   t=T/4

t=T/2   t=3T/4

a

t=0   t=T/4

t=T/2   t=3T/4

b

Fig. 5. *Simulated surface current distribution on the patch*
(a) State I, *(b)* State II

As a result of the bandpass feature of the coupled resonator pairs, the proposed antenna demonstrates a filtering performance, as shown in Fig. 6. Its S_{11} and gain as a function of frequency are compared with those of a traditional CP antenna, which has the same configuration of the patch radiator with a dual feed but without the integrated coupled resonator pairs. For both LHCP and RHCP polarization, the proposed antenna exhibits higher frequency selectivity and flatter in-band gain. The out-of-band rejection has been improved by 15.1 dB at 2.26 GHz and 12.3 dB at 2.62 GHz, 100 MHz lower/higher than the

passband edges. Two reflection zeros are evident in the $|S_{11}|$ curve indicating the 2nd-order filtering characteristics. Compared with the traditional CP antenna, the simulated maximum gain of the filtering CP antenna is 7.3 dBic, which is 0.9 dB lower due to the insertion loss of the filtering circuits and PIN diodes.
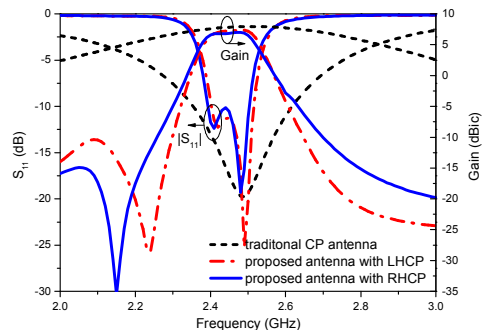

Fig. 6. *Simulated $|S_{11}|$ and gain as a function of frequency of the proposed filtering CP antenna in comparison with a traditional CP antenna*
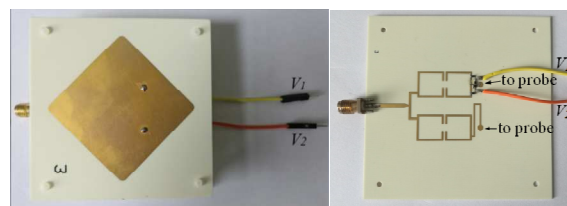
3. Results and discussion

Fig. 7. *Photograph of the fabricated reconfigurable filtering CP antenna*

To verify the design concept, a prototype filtering CP antenna is designed, fabricated and measured. Reflection coefficients are measured using an Agilent 8361C network analyzer, and the radiation patterns, axial ratios (AR) and antenna gains are measured using a SATIMO SG24 near-field measurement system.

The fabricated antenna prototype is shown in Fig. 7. The measured reflection coefficients and gains for both states are shown in Fig. 8 and in good agreement with simulations. The impedance bandwidth ($|S_{11}| < -10$ dB) is 4.5% (2.42 - 2.53 GHz) for both the LHCP and RHCP modes. The measured gain curves of the LHCP and RHCP are desirably flat across the passbands with average gains of 6.0 dBic/6.1 dBic and maximum gains of 6.4 dBic/6.5 dBic, respectively. Compared with the simulation, the measured maximum gain is about 0.9 dB lower, which is largely attributed to the losses from the SMA connector and the PIN diodes and assembly errors that are not fully accounted for. At 100 MHz outside the passband, the measured rejection is over 13.9 dB at 2.32 GHz and 10.8 dB at 2.63 GHz for the LHCP and RHCP.

Fig. 9 shows the measured and simulated AR for the LHCP and RHCP modes. The measured AR bandwidth for the LHCP is 9.4% from 2.34 to 2.57 GHz and this is 10.5%

Table 3 Comparison of the performances of polarization reconfigurable antennas

| Reference	Frequency (GHz)	Overlapped AR bandwidth	Peak gain (dBic)	Filtering response	Architecture
[5]	2.45	7%	8.7	No	Reconfigurable E-shaped patch antenna
[6]	2.44	0.72%	5.94*	No	Reconfigurable slot-etched circular microstrip antenna
[7]	2.32	19.8%	2.5	No	Monopole patch with reconfigurable slot-etched ground
[8]	4.8	12.7%	7.5	No	Reconfigurable loop antenna
[9]	5.8	0.8%	6.02	No	Patch antenna with reconfigurable feeding network
[10]	5	13.1%	11.2	No	Partially reflective surface antenna with reconfigurable power divider
[11]	1.675	23.5%	4.8	No	Four radiation arms with reconfigurable power divider
This work	2.47	9.4%	6.4	Yes	Patch antenna with phase-reconfigurable filtering structure

* The unit of peak gain in [6] is dBi.
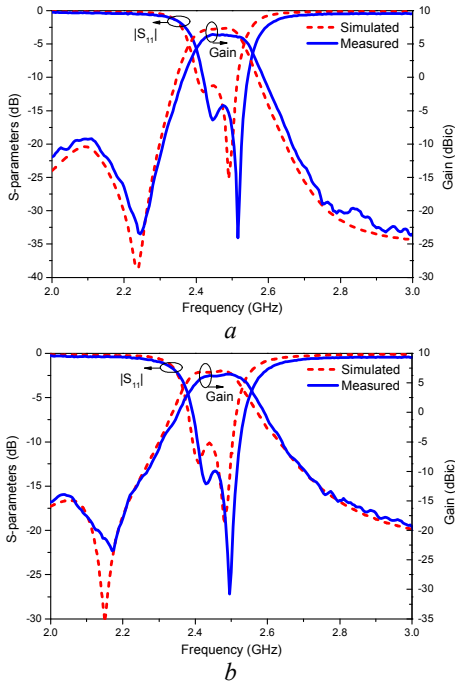
Fig. 8. *Measured and simulated reflection coefficients and gains*
(a) State I for LHCP, *(b)* State II for RHCP

Fig. 9. *Measured and simulated axial ratios*
(a) State I for LHCP, *(b)* State II for RHCP

from 2.35 to 2.61 GHz for the RHCP. The overlapping AR bandwidth for both modes is 9.4% from 2.35 to 2.57 GHz. The discrepancy of AR is caused by unaccounted parasitic in the PIN diode modeling.

Fig. 10 presents the measured normalized radiation patterns at 2.46 GHz. It has been observed but not shown here that stable broadside radiations for both the LHCP and RHCP are achieved across the passband. The measured co-polarization in the boresight is over 16.5 dB higher than the corresponding cross-polarization, and the measured front-to-back ratio is over 19 dB across the operation band. The 3-dB beam-widths in the φ=0° and 90° patterns are 58° and 68°.
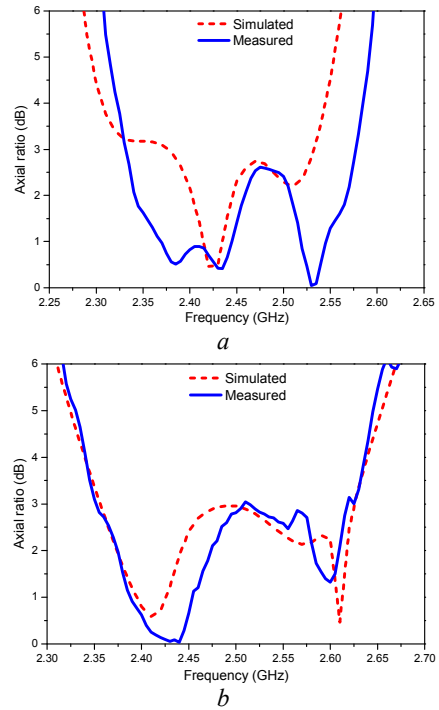
Table 3 compares the performance of this design with several other published polarization reconfigurable CP antennas. The proposed antenna has the unique combination of integrated filtering characteristics and switchable polarization. The antenna shows higher frequency selectivity and out-of-band rejection than the other designs, while maintaining good and comparable radiation performances for both the LHCP and RHCP modes. A decent AR bandwidth is achieved but there is room for improvement as compared with the wideband designs.
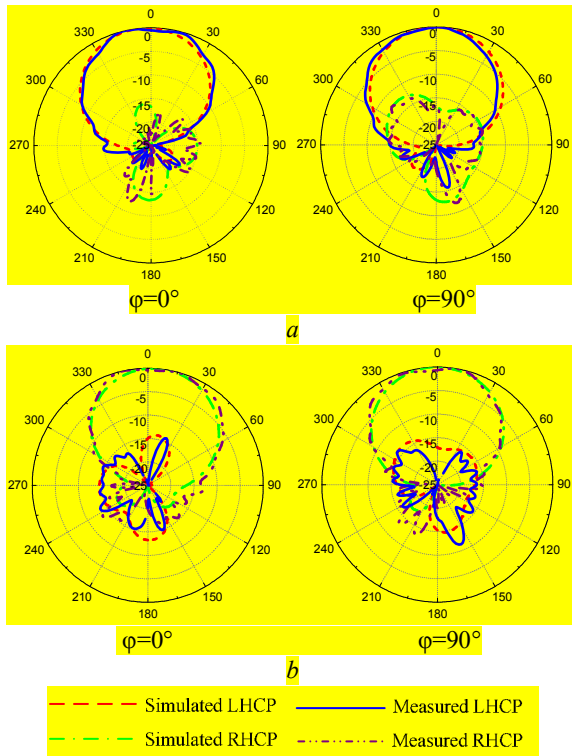
φ=0°   φ=90°

a

φ=0°   φ=90°

b

— — — Simulated LHCP   ——— Measured LHCP

—·—· Simulated RHCP   —··—·· Measured RHCP

Fig. 10. *Radiation patterns*
(a) 2.46 GHz at State I, *(b)* 2.46 GHz at State II

4. Conclusion

A new design of filtering and reconfigurable circular polarization antenna is proposed and studied in this paper. A phase-reconfigurable filtering structure is examined in detail and applied to generate the desired phase difference to feed the patch antenna. A 2nd order filtering characteristic and circular polarization are simultaneously realized. It has also been shown that the proposed antenna is capable of switching its polarization between LHCP and RHCP by using PIN diodes. A prototype operating at 2.45 GHz is designed, fabricated and measured. The multifunctional antenna offers good frequency selectivity, high out-of-band rejection, good AR bandwidth and stable in-band gain when it operates at the different polarization modes. The measurement results validate the design concept of using the phase reconfigurable filtering structures to realize polarization reconfigurable and integrated filtering CP antennas.

5. Acknowledgments

6. References

[1] Gao, S., Sambell, A., Zhong, S. S.: 'Polarization-agile antennas', IEEE Antennas Propag. Mag., 2006, 48, (3), pp. 28–37

[2] Kovitz, J.M., Rajagopalan, H., Rahmat-Samii, Y.: 'Circularly polarised half E-shaped patch antenna: a compact and fabrication-friendly design', IET Microw. Antennas Propag., 2016, 10, (9), pp. 932-938

[3] Sun, H., Sun, S: 'A novel reconfigurable feeding network for quad-polarization agile antenna design', IEEE Trans. Antennas Propagat., 2016, 64, (1), pp. 311-316

[4] Row, J.S., Chan, M.C.: 'Reconfigurable circularly-polarized patch antenna with conical beam', IEEE Trans. Antennas Propag., 2010, 58, (8), pp. 2753–2757

[5] Khidre, A., Lee, K. F., Yang, F., et al.: "Circular polarization reconfigurable wideband E-shaped patch antenna for wireless applications," IEEE Trans. Antennas Propag., 2013, 61, (2), pp. 960–964

[6] Kim, B., Pan, B., Nikolaou, S., et al.: 'A novel single-feed circular microstrip antenna with reconfigurable polarization capability', IEEE Trans. Antennas Propag., 2008, 56, (3), pp. 630–638

[7] Cai, Y.-M., Gao, S., Yin, Y., et al.: 'Compact-size low-profile wideband circularly polarized omnidirectional patch antenna with reconfigurable polarizations', IEEE Trans. Antennas Propag., 2016, 64, (5), pp. 2016–2021

[8] Zhang, L., Gao, S., Luo, Q., et al.: 'Wideband loop antenna with electronically switchable circular polarization', IEEE Antenna Wireless Propag. Lett., 2017, 16, pp. 242-245

[9] Aïssat, H., Cirio, L., Grzeskowiak, M., et al.: 'Reconfigurable circularly polarized antenna for short-range communication systems', IEEE Trans. Microw. Theory Techn., 2006, 54, (6), pp. 2856–2863

[10] Ji, L.-Y., Qin, P.-Y., Guo, Y. J., et al.: 'A wideband polarization reconfigurable antenna with partially reflective surface', IEEE Trans. Antennas Propag., 2016, 64, (10), pp. 4534–4538

[11] Lin, W., Wong, H.: 'Wideband circular polarization reconfigurable antenna', IEEE Trans. Antennas Propag., 2015, 63, (12), pp. 5938–5944

[12] Mao, C.-X., Gao, S., Y. Wang, et al.: 'Multimode resonator-fed dual-polarized antenna array with enhanced bandwidth and selectivity', IEEE Trans. Antennas Propag., 2015, 63, (12), pp. 5492–5499

[13] Zuo, J.-H., Chen, X.-W., Han, G.-R., et al.: 'An integrated approach to RF antenna-filter co-design', IEEE Antennas Wireless Propag. Lett., 2009, 8, pp. 141–144

[14] Hsieh, C.-Y., Wu, C.-H., Ma, T.-G.: 'A compact dual-band filtering patch antenna using step impedance resonators', IEEE Antennas Wireless Propag. Lett., 2015, 14, pp. 1056–1059

[15] Yusuf, Y., Gong. X.: 'Integration of three-dimensional high-Q filters with aperture antennas and bandwidth enhancement utilising surface waves', IET Microw. Antennas Propag., 2013, 7, (7), pp. 468-475

[16] Mao, C.-X., Gao, S., Y. Wang, et al.: 'An integrated filtering antenna array with high selectivity and harmonics suppression', IEEE Trans. Microw. Theory Techn., 2016, 64, (6), pp. 1798–1805

[17] Zhang, X.Y., Zhang, Y., Pan, Y.-M., et al.: 'Low-profile dual-band filtering patch antenna and its application to LTE MIMO system', IEEE Trans. Antennas Propag., 2017, 65, (1), pp. 103–113

[18] Barbuto, M., Trotta, F., Bilotti, F., et al.: 'A combined bandpass filter and polarization transformer for horn antennas', IEEE Antennas Wireless Propag. Lett., 2013, 12, pp. 1065–1068

[19] Jiang, Z. H., Werner, D. H.: 'A compact, wideband circularly polarized co-designed filtering antenna and its application for wearable devices with low SAR', IEEE Trans. Antennas Propag., 2015, 63, (9), pp. 3808–3818

[20] Li, Y.C., Xue, Q., Zhang, X.Y.: 'Single- and dual-band power dividers integrated with bandpass filters', IEEE Trans. Microw. Theory Techn., 2013, 61, (1), pp. 69–76

[21] Pozar, D. M.: 'Microwave engineering' (Wiley, 2006)

[22] Lu, Y.-L., Wang, Y., Hua, C., et al.: 'Design of compact filtering rat-race hybrid with λ/2-resonators', Electron. Lett., 2016, 52, (21), pp. 1780-1782

[23] Hennings, A., Semouchkina, E., Baker, A., et al.: 'Design optimization and implementation of bandpass filters with normally fed microstrip resonators loaded by high-permittivity dielectric', IEEE Trans. Microw. Theory Techn., 2006, 54, (3), pp. 1253–1261